Since January 2020 Elsevier has created a COVID-19 resource centre with free information in English and Mandarin on the novel coronavirus COVID-19. The COVID-19 resource centre is hosted on Elsevier Connect, the company's public news and information website.

Computational Toxicology 15 (2020) 100127

Contents lists available at ScienceDirect

Computational Toxicology

journal homepage: www.elsevier.com/locate/comtox

The Se···S/N interactions as a possible mechanism of δ-aminolevulinic acid dehydratase enzyme inhibition by organoselenium compounds: A computational study

Pablo Andrei Nogara[a], Laura Orian[b], João Batista Teixeira Rocha[a,*]

[a] Departamento de Bioquímica e Biologia Molecular, Universidade Federal de Santa Maria (UFSM), Santa Maria 97105-900, RS, Brazil
[b] Dipartimento di Scienze Chimiche, Università degli Studi di Padova, Via Marzolo 1, 35131 Padova, Italy

ARTICLE INFO

Keywords:
Porphobilinogen synthase
Protein homology modeling
Docking
DFT calculations
In silico analysis

ABSTRACT

Organoselenium compounds present many pharmacological properties and are promising drugs. However, toxicological effects associated with inhibition of thiol-containing enzymes, such as the δ-aminolevulinic acid dehydratase (δ-AlaD), have been described. The molecular mechanism(s) by which they inhibit thiol-containing enzymes at the atomic level, is still not well known. The use of computational methods to understand the physical–chemical properties and biological activity of chemicals is essential to the rational design of new drugs. In this work, we propose an *in silico* study to understand the δ-AlaD inhibition mechanism by diphenyl diselenide (DPDS) and its putative metabolite, phenylseleninic acid (PSA), using δ-AlaD enzymes from *Homo sapiens* (*Hs*δ-AlaD), *Drosophila melanogaster* (*Dm*δ-AlaD) and *Cucumis sativus* (*Cs*δ-AlaD). Protein modeling homology, molecular docking, and DFT calculations are combined in this study. According to the molecular docking, DPDS and PSA might bind in the *Hs*δ-AlaD and *Dm*δ-AlaD active sites interacting with the cysteine residues by Se···S interactions. On the other hand, the DPDS does not access the active site of the *Cs*δ-AlaD (a non-thiol protein), while the PSA interacts with the amino acids residues from the active site, such as the Lys291. These interactions might lead to the formation of a covalent bond, and consequently, to the enzyme inhibition. In fact, DFT calculations (mPW1PW91/def2TZVP) demonstrated that the selenylamide bond formation is energetically favored. The *in silico* data showed here are in accordance with previous experimental studies, and help us to understand the reactivity and biological activity of organoselenium compounds.

1. Introduction

The utilization of selenium (Se) in organic synthesis has been producing a vast number of organoselenium compounds since the second half of the 19th century. For instance, Ebselen (EBS) was synthesized in 1924, and nowadays is the most investigated of the organoselenium compounds (Fig. 1A) [1]. Diphenyl diselenide (DPDS) is the simplest diaryl diselenide and has been tested as a pharmacological agent [2]. The organoselenium derivatives present many pharmacological properties, such as anti-inflammatory, cardioprotective, neuroprotective, and antioxidant, this last one due to their ability to reduce hydrogen peroxide (H_2O_2) to water (H_2O). Therefore, these compounds are considered mimetics of the glutathione peroxidase (GPx) enzyme and are promising drugs [3–6].

In addition, EBS and DPDS can oxidize thiol groups of proteins [3,4,7] as observed in the mammalian enzyme δ-aminolevulinic acid dehydratase (*m*δ-AlaD) or porphobilinogen synthase (PBGS) (EC 4.2.1.24). Since the δ-AlaD is an important enzyme involved in the porphyrins' synthesis, its inhibition can have toxicological consequences [8–11]. The δ-AlaD catalyzes the asymmetric condensation of two molecules of 5-aminolevulinic acid (δ-aminolevulinic acid – 5-Ala), forming the porphobilinogen (PBG), which is the precursor of porphyrins' synthesis (Fig. 1B). In the enzyme active site, each substrate binds at two different subsites (A and P), leading to the regioselective product PBG. The acetic acid and propanoic acid side-chains of PBG originate from the subsites A and P, respectively [12–14]. Porphyrins are essential to living beings, particularly to the aerobic life, due to the heme prosthetic group, which is involved in the transport of oxygen (hemoglobin and myoglobin), xenobiotic metabolism (cytochrome P450), protection against peroxides (peroxidases and catalases), and chlorophyll synthesis [13,15–17]. There are two major classes of δ-AlaD: the Zn-dependent enzymes (that are present in mammals, fungi

* Corresponding author.
E-mail address: jbtrocha@yahoo.com.br (J.B.T. Rocha).

https://doi.org/10.1016/j.comtox.2020.100127
Received 3 March 2020; Received in revised form 29 May 2020; Accepted 3 June 2020
Available online 09 June 2020

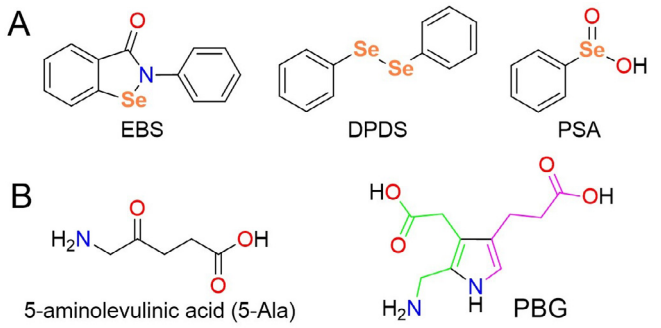

Fig. 1. (A) The structural formula of some organoselenium compounds, (B) the 5-aminolevulinic acid (5-Ala) substrate and porphobilinogen (PBG) product of the δ-AlaD.

and some bacteria, such as *Escherichia coli*) [15,18,19], and the Mg-dependent enzymes, that are found mainly in plants, protozoa and other bacteria [13,20–22].

Studies have demonstrated that the DPDS can inhibit the δ-AlaD enzyme from human (*Hs*δ-AlaD) and rodents [10,11,23–28]. The δ-AlaD from *Drosophila melanogaster* (*Dm*δ-AlaD) can also be inhibited by DPDS [29]. In contrast, DPDS do not inhibit δ-AlaD from cucumber, *Cucumis sativus* (*Cs*δ-AlaD); nevertheless, its putative metabolite, the phenylseleninic acid (PSA), can inhibit the *Cs*δ-AlaD [30]. In fact, the toxicity of organoselenium compounds could be associated with their metabolic oxidation by flavin-containing monooxygenases [4,31,32]. However, the inhibition mechanism(s) involved in these cases has not been established yet.

To complement and better understand the *in vivo* and *in vitro* data, *in silico* methods have been used to analyze, simulate, and predict the pharmacology and toxicity of chemicals [33–37]. There are many types of computational methods, where the molecular docking stands out by simulating the interactions between macromolecules (proteins and DNA) and ligands (substrate, inhibitor, and agonist). This method consists in predicting the binding mode of the ligand at the binding site of a given target, in addition to the estimation of affinity for the receptor, by predicting binding free energy (ΔG) [38–41]. Quantum mechanical methods, such as the density functional theory (DFT) approach, are frequently used in the study of structures, reactions, and molecular properties [42–44], but are strictly limited to systems of few hundreds of atoms. In addition, the protein homology modeling has been successfully employed to predict the 3D protein structure, which is essential in many cases when the tertiary or quaternary structure must be studied [45–49].

Different *in silico* methods have been adopted to predict the reactivity, toxicity, and pharmacology of organoselenium compounds and selenoproteins [44,50–58]. Here, to better understand the toxicological effects of organoselenium molecules, and how they interact with target proteins, we propose an *in silico* approach combining protein homology modeling, molecular docking simulations, and DFT calculations (Scheme 1). Based on the difference of DPDS and PSA inhibition behavior on δ-AlaD enzymes, this study aims to compare the intermolecular interactions between the *Hs*δ-AlaD, *Dm*δ-AlaD and *Cs*δ-AlaD enzymes and the DPDS and PSA organoselenium compounds, to gain insight into their mechanisms of inhibition.

2. Materials and methods

2.1. Protein homology modeling

First, the homology analysis of the primary structure of δ-AlaD enzymes from cucumber (*Cucumis sativus*), fruit fly (*Drosophila melanogaster*), human (*Homo sapiens*), mouse (*Mus musculus*), zebrafish (*Danio rerio*), cockroach (*Blattella germanica*), protozoa (*Toxoplasma gondii*), yeast (*Saccharomyces cerevisiae*), archaeon (*Pyrobaculum calidifontis*) and bacteria (*Chlorobaculum parvum*, *Escherichia coli*, *Pseudomonas aeruginosa*, *Staphylococcus aureus* and *Wolbachia*) were performed. The FASTA amino acid sequences for δ-AlaD enzymes were obtained from the the National Center for Biotechnology Information – NCBI (https://www.ncbi.nlm.nih.gov/pubmed/), UniProt (http://www.uniprot.org/) and Protein Data Bank – PDB (http://www.rcsb.org/pdb), according to the respective codes: *Blattella germanica*: UniProt (A0A2P8XHW3_BLAGE); *Chlorobaculum parvum*: PDB (2C1H); *Cucumis sativus*: UniProt (A0A0A0LQK9_CUCSA); *Danio rerio*: NCBI (NP_001017645.1); *Drosophila melanogaster*: UniProt (Q9VTV9_DROME); *Escherichia coli*: PDB (1L6S); *Homo sapiens*: PDB (1E51); *Mus musculus*: NCBI (NP_001263375.1); *Pseudomonas aeruginosa*: PDB (1GZG); *Pyrobaculum calidifontis*: PDB (5LZL); *Saccharomyces cerevisiae*: PDB (1H7N); *Staphylococcus aureus*: UniProt (HEM2_STAAR); *Toxoplasma gondii*: PDB (3OBK); *Wolbachia*: NCBI (WP_041571452.1). Regarding of FASTA from PDB, it was used the FASTA associated with the corresponding PDB file on the database (we do not extract the FASTA from the PDB file). The Clustal Omega server (http://www.ebi.ac.uk/Tools/msa/clustalo) was used to make the multiple sequence alignment, and the similarity between the δ-AlaD sequences was calculated from the Geneious program (https://www.geneious.com) (Fig. 2, S1, S2 and Table S1).

Since there is no available three-dimensional structure of *Dm*δ-AlaD and *Cs*δ-AlaD, the Swiss-Model (https://swissmodel.expasy.org) [59], Phyre2 [60], and Geno3D servers [61] were used to obtain their structures, using the amino acid sequence of the *Cucumis sativus* and *Drosophila melanogaster* δ-AlaD, taken from UniProt with the codes A0A0A0LQK9_CUCSA and Q9VTV9_DROME, respectively. The 3D structures of the *Chlorobaculum parvum* (PDB: 2C1H [62]), *Pseudomonas aeruginosa* (PDB: 1GZG [63]), and *Toxoplasma gondii* (PDB: 3OBK [21]) where used as template to build the *Cs*δ-AlaD models, while the *Escherichia coli* (PDB: 1L6S [64]), *Pyrobaculum calidifontis* (PDB: 5LZL [18]), and *Saccharomyces cerevisiae* (PDB: 1H7N [19]) structures where used as template to build the *Dm*δ-AlaD models. The validation of the protein models were carried out by the programs: Verify 3D [65,66], ProSA [67], PROCHECK [68,69], and ERRAT [70]. The Ramachandran plot was made by the PDBsum server (www.ebi.ac.uk/pdbsum/) [71]. More details can be found in the Supporting information.

2.2. Molecular docking

To carry out the docking simulations, the *Hs*δ-AlaD was obtained from PDB with the code 1E51 [72], and the *Dm*δ-AlaD-1L6S and *Cs*δ-AlaD-3OBK models were obtained from protein homology modeling by the Swiss-model program (as described above). The CHIMERA 1.8 program [73] was used to add the hydrogen atoms to the proteins. The Lys199/195/291 and Lys252/248/344 residues were considered neutral (deprotonated) [14], which was confirmed by H++ analysis (http://biophysics.cs.vt.edu). The ligands (PBG and the organoselenium compounds) were built in the Avogadro 1.1.1 software [74], followed by a geometric optimization using the MOPAC program (http://openmopac.net/MOPAC2012.html) with the semi-empirical method PM6 (with the water dielectric constant) [75]. The PSA was considered deprotonated (pka = 4.79) [76] during the docking simulations. The protein and ligands were converted to the *pdbqt* format with the AutoDockTools [77], with the Gasteiger and MOPAC charges, respectively. The partial charge (0.302) of the Zn^{2+} ion from *Hs*δ-AlaD and *Dm*δ-AlaD were obtained from a previous study [51].

The AutoDockVina 1.1.1 software [78] was used for the docking simulations, with exhaustiveness of 100. The best docking protocol was obtained using the ligands and the side chain of Arg209 and Lys252 residues from *Hs*δ-AlaD (Arg205 and Lys248 from *Dm*δ-AlaD-1L6S, and Arg301 and Lys344 from *Cs*δ-AlaD-3OBK) flexible. The grid boxes (with spacing of 1 Å) were centered in the active site of the enzymes *Hs*δ-AlaD (coordinates: x = 31.63; y = 73.65; z = 57.08), *Dm*δ-AlaD-1L6S

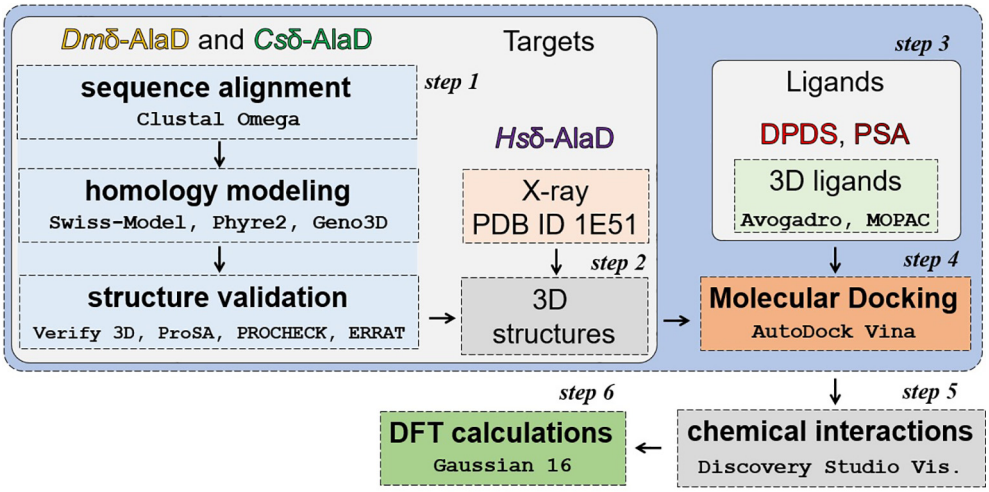

Scheme 1. Overview of all the steps involved in this study.

(coordinates: x = 19.72; y = 83.35; z = 52.14), and *Cs*δ-AlaD-3OBK (coordinates: x = -64.60; y = -77.40; z = 28.05), with a size of 25 × 25 × 25 Å, in both cases. The Discovery Studio Visualizer 17.2.0. (DSV) program (https://www.3dsbiovia.com/) was used to analyze the results, where the conformers of lowest binding free energy (ΔG) were selected as the best model. The molecular docking protocols were validated by the RMSD (root-mean-square deviation) values from the PBG molecules, which give the relationship between the experimental and the theoretical data in a receptor-ligand complex. RMSD values lower than 2.0 Å indicate good quality of data reproduction (Fig. S4) [41,79,80] (details can be found in the Supporting Information).

2.3. Density functional theory calculations

All quantum chemistry calculations have been performed using density functional theory (DFT) approach as implemented in Gaussian 09 rev. E.01 program [81]. mPW1PW91 (Perdew-Wang hybrid functional) [82] was used, in combination with the def2TZVP (Triple zeta quality with polarization functions) basis set for all the atoms [83,84].Full geometry optimizations were carried out in gas phase; solvation (water) effects were taken into account in subsequent single point calculations at the same level of theory using PCM approximation [85].

3. Results and discussion

3.1. Protein sequence comparison and homology modeling

Considering that DPDS inhibits the *Hs*δ-AlaD [11] and *Dm*δ-AlaD [29] and does not inhibit *Cs*δ-AlaD [30], we initially compared the primary structure of the δ-AlaD enzymes (including other different species) through multiple sequence alignment (Fig. 2, Fig. S1/S2 and Table S1). The analysis of the sequence alignment data demonstrated that are two groups of proteins, i.e. Group A, which includes the species that present Cys residues in the active site (*Saccharomyces cerevisiae, Drosophila melanogaster, Danio rerio, Homo sapiens, Mus musculus, Escherichia coli, Pyrobaculum calidifontis and Staphylococcus aureus*), and Group B, which includes the species that have Asp residues (*Toxoplasma gondii, Cucumis sativus, Wolbachia, Pseudomonas aeruginosa* and *Chlorobaculum parvum*) (Fig. S2). Interestingly, the *Blattella germanica* δ-AlaD is small when compared to the other species (146 *vs* ~ 330 residues) and has not the Cys region of the active site; however, the catalytic Lys residues are conserved (Fig. S1). According to the phylogenetic tree (Fig. S2) it belongs to Group A.

In general, the three cysteine residues from the active site of Group A δ-AlaD were replaced by two aspartate residues and one alanine residue in Group B (Fig. 2 and Fig. S1/S2) indicating a significant change in the nature of the active site. In addition, the Arg221 (in the human protein) were replaced by a Lys residue in the δ-AlaD from Group B (Lys313 in *Cs*δ-AlaD). As the Lys and Arg are basic and positively charged residues, practically, the same physical–chemical properties

```
S.cerevisiae    FGVPLIPGTKDPVGTAADDPAGPVIQGIKFIREYFPE-LYIICDVCLCEYTSHGHCGVLY 147
D.melanogaster  FGVVD-PDMKDEQASNADSAKNPVVLALPKLREWFPD-LLIACDVCICPYSSHGHCGLLG 134
B.germanica     ------------------------------------------------------------ 0
D.rerio         FGVPA-KVAKDERGSGADADDTPAVLAVKKLRSTFPE-LVLACDVCLCPYTSHGHCGILR 138
H.sapiens       FGVPS-RVPKDERGSAADSEESPAIEAIHLLRKTFPN-LLVACDVCLCPYTSHGHCGLLS 136
M.musculus      FGVPS-RVPKDEQGSAADSEDSPTIEAVRLLRKTFPS-LLVACDVCLCPYTSHGHCGLLS 136
P.calidifontis  FGVLP-DELKNPEGTGGYDPEGVVPRAIRLIKEIFGDRVLVFADVCLCEYTDHGHCGVVK 139
E.coli          FGISH---HTDETGSDAWREDGLVARMSRICKQTVPE-MIVMSDTCFCEYTSHGHCGVLC 133
S.aureus        FGVPN---SKDDIGTGAYIHDGVIQQATRIAKKMYDD-LLIVADTCLCEYTDHGHCGVID 132
T.gondii        FPKVD-DELKSVMAEESYNPDGLLPRAIMALKEAFPD-VLLLADVALDPYSSMGHDGVVD 150
Wolbachia       FPVVD-SKLKSENAEEAYNSDNLICKAIRAIKLKVPG-IGIIADVALDPYTTHGHDGILK 137
C.sativus       FPKVP-DALKTPTGDEAYNDNGLVPRTIRLLKDKYPD-LVIYTDVALDPYSSDGHDGIVR 229
C.parvum        FGIP---EQKTEDGSEAYNDNGILQQAIRAIKKAVPE-LCIMTDVALDPFTPFGHDGLVK 139
P.aeruginosa    FPVTP-VEKKSLDAAEAYNPEGIAQRATRALRERFPE-LGIITDVALDPFTTHGQNGILD 143
```

Fig. 2. Multiple alignments of the δ-AlaD amino acids sequence of different organisms. Only a fragment from the active site of the proteins are shown. The residues from the active site are highlighted: Cys (yellow); residues that remain conserved (cyan), residues that are not conserved when compared to the human enzyme (green and pink). The complete alignment is shown in Fig. S1. (For interpretation of the references to color in this figure legend, the reader is referred to the web version of this article.)

are conserved. These observations are in accordance with previous studies of Kervinen et al. (2001) [86] where five δ-AlaD enzymes (from *Pisum sativum*, *Pseudomonas aeruginosa*, *Bradyrhizobium japonicum*, *Escherichia coli,* and *H. sapiens*) sequences were analysed, and the metal-binding region determined.

Here, based on these observations, we can suppose that DPDS does not inhibit the *Cs*δ-AlaD because this enzyme does not present Cys residues in its active site. However, it does not explain why PSA inhibits the *Cs*δ-AlaD. For a better understanding of the interactions between inhibitors and enzymes, the molecular docking simulations were performed. Taking into account that there are no *Cs*δ-AlaD and *Dm*δ-AlaD structures available, the 3D model of these enzymes were built using protein homology modelling.

Homology modeling is the most accurate method to build protein structure models [87–89]. Among the different programs developed for this purpose, in this study we have chosen the Swiss-Model [59], Phyre2 [60], and Geno3D [61] to create the *Dm*δ-AlaD and *Cs*δ-AlaD structures. Taking in account the primary structure similarity between the δ-AlaD enzymes (Fig. 2, Figs. S1–S2 and Table S1), three templates were selected for *Dm*δ-AlaD (PDB ID: 1H7N, 1L6S and 5LZL) and three for *Cs*δ-AlaD (PDB ID: 1GZG, 2C1H, and 3OBK). Each template was used in the protein homology modeling with the three programs above cited, to find the best protein model. The 3D structure models of *Dm*δ-AlaD and *Cs*δ-AlaD built were validated using the programs: Verify 3D [65,66], ProSA [67], PROCHECK [68,69], and ERRAT [70] (Tables S1–S2).

According to the data in Tables S2 and S3, the best *Dm*δ-AlaD and *Cs*δ-AlaD models were obtained from the PDB ID 1L6S and PDB ID 3OBK templates, respectively, using the Swiss-Model program, which turned out to be the most performant program for this task. *Dm*δ-AlaD-1L6S and *Cs*δ-AlaD-3OBK models showed a satisfactory protein structure, because the validation parameters are in the range of native protein structure (see the Supporting information), and they were used for the molecular docking simulations.

Despite the differences in the primary structure between the *Homo sapiens* δ-AlaD, *Dm*δ-AlaD and *Cs*δ-AlaD, the comparison of the tertiary structure of the three enzymes exhibited a very similar organization of the residues, with the simulated PBG binding pose presenting practically the same conformation and interactions (Fig. 3). Here, we highlighted the major difference in the active site of both enzymes. As shown in Fig. 3AB, in *Hs*δ-AlaD and *Dm*δ-AlaD the thiolates of the Cys residues are coordinated to a zinc ion (Zn^{2+}), where this metal nucleus acts as a Lewis acid and Zn···N coordination with the amino moiety (Lewis base) from PBG is formed. This Zn···N interaction is essential to the catalysis of the δ-AlaD, because it specifically guides one molecule of 5-Ala substrate in subsite A, before the cyclization to pyrrole ring [86,90]. In fact, the Cys mutations cause a dramatic reduction in the enzyme activity [12]. On the other hand, according to the docking simulation between the PBG and *Cs*δ-AlaD, the orientation of one molecule of 5-Ala substrate is likely driven by the H-bonds between the amino moiety from 5-Ala and the carboxylate groups of Asp217 and Asp225 residues (Fig. 3C). The PBG binding pose obtained by the docking in *Cs*δ-AlaD is very similar to the crystallographic data collected from *T. gondii* δ-AlaD [21]. Interestingly, Asp217 and Asp225 are the residues that correspond to Cys124 and Cys132 residues in the human enzyme, respectively (Figs. 2 and 3).

In addition, in the case of *Cs*δ-AlaD, the Mg^{2+} ion is not present in the active site (Fig. 3C), and does not participate directly in the catalysis. However, the Mg^{2+} is essential to enzyme function, as observed in *E. coli*, *Bradyrhizobium japonicum*, *Pseudomonas aeruginosa,* and *P. sativum,* due to the H-bonding network around this metal ion maintaining the quaternary structure of δ-AlaD [13–15,86]. This difference in the active site of δ-AlaD from different species must be taken into account in the design of selective inhibitors with useful applications, such as in the case of δ-AlaD from *Wolbachia* [91–93] and *Staphylococcus aureus* [94]. Moreover, due to the similarity of the active site from δ-AlaD of the group B, the use of plant δ-AlaD (such as cucumber) can provide a simple, practical and cheap *in vitro* assay to find new selective inhibitors.

3.2. Organoselenium molecular docking study

Molecular docking simulations were carried out to understand the δ-AlaD inhibition by DPDS and PSA. According to the docking between the *Hs*δ-AlaD and DPDS, this latter interacts with the enzyme active site mainly by hydrophobic interactions (π-π stacking with Phe79, Tyr205 and Phe208 residues and alkyl-π with Pro125). The selenium atoms of DPDS interact with the carboxylic group of Asp120 and with the Zn^{2+} ion, besides the thiolate group from Cys124 (Fig. 4A). The putative DPDS metabolite, PSA, also interacts in the *Hs*δ-AlaD active site, by π-π stacking with Tyr205 and Phe208, H-bond with Ser168, and interactions with Tyr196 (anion-π interaction between the seleninate and the phenyl moieties), Asp120 (repulsive electrostatic interaction between the seleninate and carboxyl groups), and zinc ion (coordination). In addition, Se···S interaction with Cys124 is observed (Fig. 4B).

The simulation of DPDS with the *Dm*δ-AlaD demonstrated that this organoselenium compound could access the active site making hydrophobic interactions with Arg205, Pro212 (alkyl and phenyl groups), Phe204 and Tyr201 (phenyl and phenyl moieties), besides interacting with Arg217 via H-bond (selenyl and guanidinyl groups [95,96]) (Fig. 4C). In addition, the DPDS showed a Se···S interaction with Cys122. The PSA molecule also binds in the *Dm*δ-AlaD active site, through hydrophobic π-π stacking with Phe204 and Tyr201 (phenyl and phenyl moieties), through H-bonds with Ser165, Lys195, and Gln221 (seleninate and OH, NH and C=O groups, respectively), and Zn···O coordination. Similarly to DPDS, the PSA also showed Se···S interaction with Cys122 (Fig. 4D).

On the other hand, the docking simulations between the *Cs*δ-AlaD and DPDS demonstrated that it does not enter in the *Cs*δ-AlaD active site. In fact, DPDS binds in the superficial region of the enzyme, close to the entrance of the active site, interacting with the Lys313 (phenyl and carbon chain) and presenting an intramolecular π-π stacking (phenyl-phenyl) (Fig. 4E). In contrast, PSA can access the active site of *Cs*δ-AlaD (Fig. 4F), making H-bonds with Arg301 and Lys291 residues, stabilized by electrostatic interaction with Asp217, and π-π stacking with Phe330 (phenyl and phenyl moieties).

Finally, we simulated the interactions of other putative oxidized organoselenium forms [97] (Fig. S5) to verify if these molecules are able to interact with the δ-AlaD enzymes, and its binding partner. For *Hs*δ-AlaD, all organoselenium molecules show Se···S interaction (3.1–5 Å) with the Cys124 residue (Fig. S6), except *R,R*-DPDS(O). Conversely, for *Dm*δ-AlaD, only *S,R*-DPDS(O), *R*-DPDS(O) and PhSeOH show Se···S interaction (4–4.4 Å) (Fig. S7). In relation of the *Cs*δ-AlaD, we verified that all the selenoxide forms of DPDS do not bind in the active site (Fig. S8), as observed with DPDS. However, like PSA, PhSeOH enters in the active site and interacts with Lys291. These data suggest that for *Cs*δ-AlaD small organoselenium electrophilic moieties can indeed inhibit the enzyme. In addition, the stereochemistry of the compounds play an essential role in the binding mode in the enzyme.

The predicted binding free energy (ΔG_{bind}) for the *Hs*δ-AlaD indicates that the interaction of DPDS with the enzyme is energetically more favored than the interaction PSA-enzyme (Table 1). In contrast, ΔG_{bind} for *Dm*δ-AlaD suggests a more favorable PSA-enzyme than DPDS enzyme binding. Similarly, in *Cs*δ-AlaD, PSA showed (negatively) larger binding energy than DPDS. Finally, the presence of oxygen atoms in the oxidized forms of DPDS enabled the formation of H-bonds facilitating thermodynamically the binding.

In the *Hs*δ-AlaD and *Dm*δ-AlaD enzymes, both PSA and DPDS presented similar binding pose, interacting with amino acid residues from the active site. Notably, Cys124 and Cys122 (*Hs*δ-AlaD and *Dm*δ-AlaD, respectively), stabilization occurs via Se···S interaction (Fig. 4A–D). However, for *Cs*δ-AlaD, only PSA binds in the active site, and no Se···S

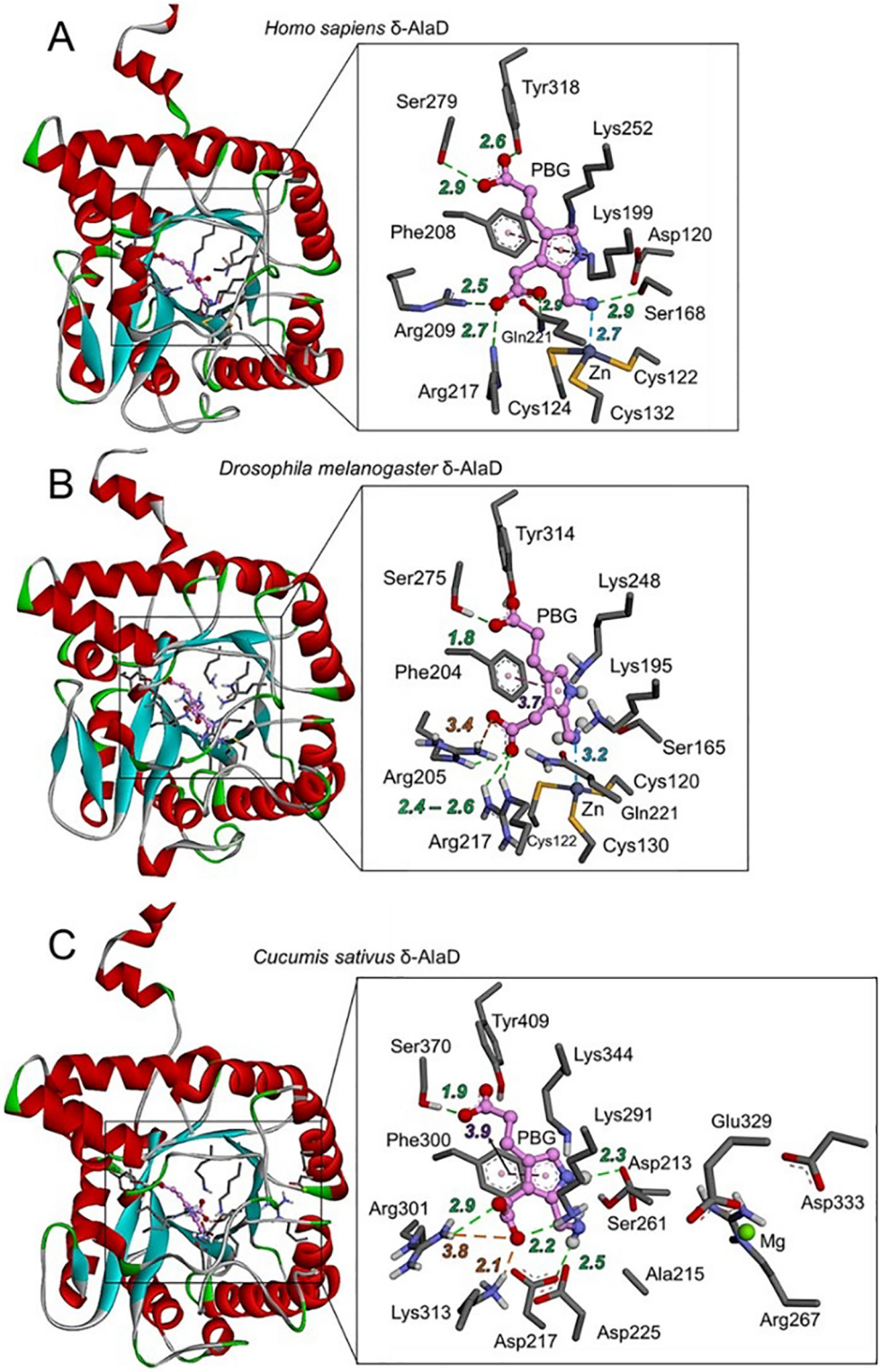

Fig. 3. Comparison between the 3D structures of δ-AlaD from *Homo sapiens* (A), *Drosophila melanogaster* (B) and *Cucumis sativus* (C). The active site is highlighted, and the carbon atoms of PBG are represented in pink color. (A) Human δ-AlaD structure from the crystal PDB ID 1E51 [72], and (B) *Dm*δ-AlaD and (C) *Cs*δ-AlaD from protein homology modeling, with the PBG binding pose from the molecular docking. The hydrogen atoms were omitted for clarity. H-bonds, electrostatic (charge-charge) and hydrophobic (π–π) interactions, besides the zinc coordination, are represented by green, orange, purple, and blue dotted lines, respectively; all distances are in Å. (For interpretation of the references to color in this figure legend, the reader is referred to the web version of this article.)

interaction is present because the *Cs*δ-AlaD does not have Cys residues in the active site (Fig. 4E–F). These outcomes strongly suggest that organoselenium compounds binding in the active sites could prevent the entrance of the substrate 5-Ala, thus inhibiting the enzymes.

The previous *in vitro* assays have indicated that the mechanism of *Hs*δ-AlaD (or mammalian δ-AlaD) and *Dm*δ-AlaD inhibition by organoselenium compounds involves Cys oxidation because dithiothreitol (DTT_{red}) could reactivate the enzyme from these sources [10,11,24,29,30,98]. The Se···S interaction could lead to the formation of the selenenyl sulfide bond (Se–S) [99,100], an adduct between the protein and the selenium compound, by means of a nucleophilic attack of the thiolate moiety of Cys124(122) to the Se atom of either DPDS or PSA. In fact, previous experimental as well as theoretical studies have indicated that Se-S bound can be easily formed between reduced thiol-containing molecules and diselenide- (Se-Se) and seleninic acid (R-SeO_2H)-containing molecules [99,101,110,102–109].

In the next step, a vicinal thiol group – from Cys122(120) and/or Cys132(130) – could perform a nucleophilic attack to the electrophilic S

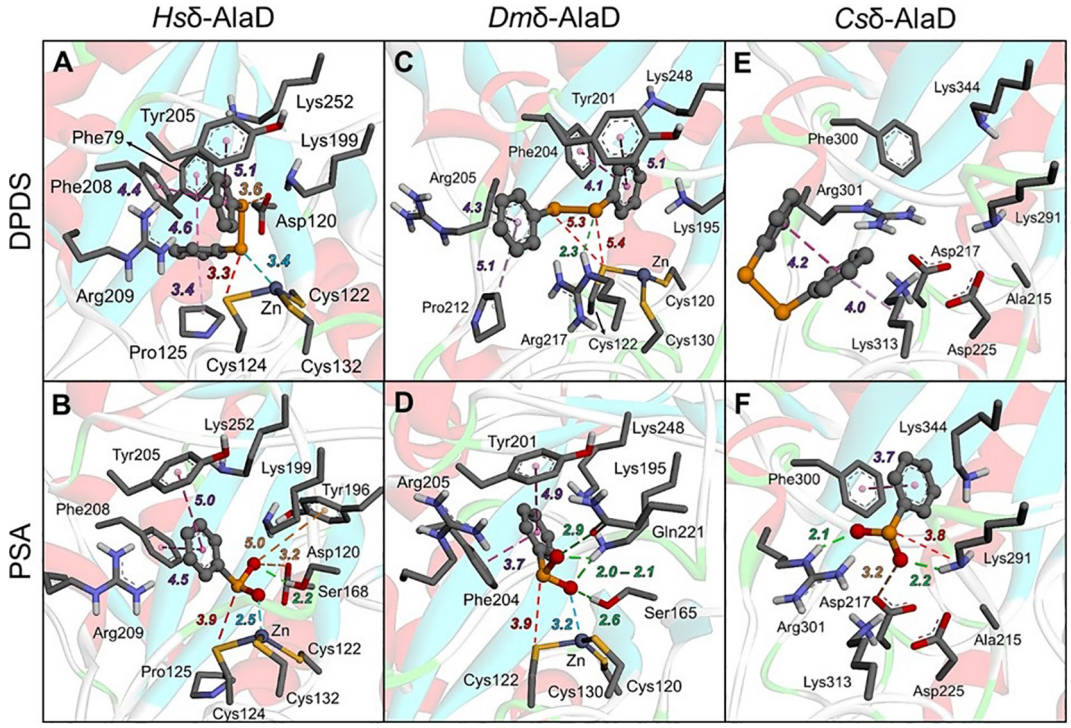

Fig. 4. Molecular docking of organoselenium compounds with *Hs*δ-AlaD (A, B), *Dm*δ-AlaD (C, D) and *Cs*δ-AlaD (E, F). (A, C, and E) DPDS binding pose in *Hs*δ-AlaD, *Dm*δ-AlaD, and *Cs*δ-AlaD enzymes, respectively. (B, D, and F) PSA binding pose in *Hs*δ-AlaD, *Dm*δ-AlaD, and *Cs*δ-AlaD, respectively. H-bonds (green), hydrophobic (π-π, alkyl-π) (purple), cation-π, anion-π, electrostatic interactions (orange), and zinc coordination (blue), are represented by dotted lines; all the distances are in Å. The ligands and the amino acids lateral chains are represented by ball and stick, and stick models, respectively. (For interpretation of the references to color in this figure legend, the reader is referred to the web version of this article.)

Table 1
Predicted ΔG_{bind} (kcal/mol) from molecular docking.

Enzyme	*Hs*δ-AlaD	*Dm*δ-AlaD	*Cs*δ-AlaD
DPDS	−6.2	−5.9	−5.2
PSA	−5.1	−6.1	−5.9
R,R-DPDS(O)	−7.0	−8.0	−5.1
S,R-DPDS(O)	−7.0	−7.9	−6.7
S,S-DPDS(O)	−6.1	−6.1	−4.8
R-DPDS(O)	−7.0	−6.5	−5.2
S-DPDS(O)	−6.3	−6.0	−5.1
PhSeOH	−4.6	−5.8	−4.8

atom of the Se–S bond, leading to the disulfide bridge (S–S) formation, i.e., thiol oxidation, and the release of zinc ion [7,99,108,111–113]. In fact, the distances between the S atoms are 3.7–4.6 Å for both *Hs*δ-AlaD and *Dm*δ-AlaD. Previous studies suggested that the cysteine oxidation (S–S) in the *Hs*δ-AlaD active site involves Cys124 and Cys132 residues. The Cys124 residue is the first thiolate that reacts with diselenides or selenides/selenoxides, forming the Se–S intermediate; then, Cys132 reacts with this intermediate leading the disulfide bridge, denaturing the active site [51,114].

*Cs*δ-AlaD has no Cys residues in the active site and consequently, the Cys oxidation mechanism is not possible. PSA, likely due to its polarity, has a better affinity for the active site of *Cs*δ-AlaD (where polar and basic residues are present). PSA has a highly electrophilic Se atom [30,115,116]. Its Hirshfeld partial charge is higher than the one computed for Se in DPDS and in the other selenium compounds of this study, indicating a deficiency of electrons (Table S4). In addition, due to the short distance between the Se atom and the amino group from Lys291 (Se···N = 3.8 Å, Fig. 4F), a nucleophilic attack from the Lys291 on PSA could occur, forming a seleninamide moiety (Ph-**Se(O)NH**-Lys), i.e., an adduct between the enzyme and the organoselenium moiety, which might inhibit the *Cs*δ-AlaD. The seleninamide formation from seleninic acid has already been reported in the literature [115,117]. The formation of seleninamide could prevent the reaction between the Lys291 residue and the 5-Ala substrate (the Schiff base formation, which is an essential step in the δ-AlaD catalytic cycle [14,15]). The *in vitro* study of Farina et al. (2002) [30] showed that in the presence of DTT_{red} the *Cs*δ-AlaD is not inhibited. A possible explanation is that the sulfur atom from DTT could react with the seleninamide adduct, forming a thioseleninate moiety (Ph-**Se(O)S**-DTT) releasing the free Lys291 and consequently reactivating the enzyme (Ph-**Se(O)NH**-Lys + DTT-**SH** → Ph-**Se(O)S**-DTT + Lys-**NH_2**). In fact, the thioseleninate intermediate can be formed via a reaction between seleninamide and thiol molecules [5,100,118,119].

The reaction between the PSA and the active site in *Cs*δ-AlaD was investigated by means of DFT calculations. For this purpose, we set up a model reaction, using $EtNH_2$ as a model of the Lys residue and PSA in the protonated form (PhSeOOH), as it should be due to its proximity to Arg301 (Fig. 4F) and because water is a better leaving group than hydroxyl anion. Our results (Fig. 5) indicate that the seleninamide formation is energetically favored, both in the gas and water phase. The reactant complex ($PhSeOOH{\cdot}EtNH_2$) is characterized by an H-bond between the hydroxyl and amino groups and by a short distance Se···N (3.8 Å), promoting the release of a water molecule and the formation of the Se–N bond in the product complex ($PhSeONHEt{\cdot}H_2O$) (Fig. 5A).

The proximity between electrophilic forms of organoselenium molecules and nucleophilic moieties from critical amino acids residues (in this case Se···S/N interactions from Cys124, Cys122, and Lys291, from *Hs*δ-AlaD, *Dm*δ-AlaD, and *Cs*δ-AlaD, respectively) could lead to covalent bonds formation, and consequently, these adducts can impair the functions of enzymes, inhibiting them. This mechanism could justify the toxicity of some organoselenium compounds.

The understanding of the mechanism of organoselenium compounds toxicity will be crucial in the designing of new molecules less toxic and more selective in relation to pharmacological targets. In this sense, the

A

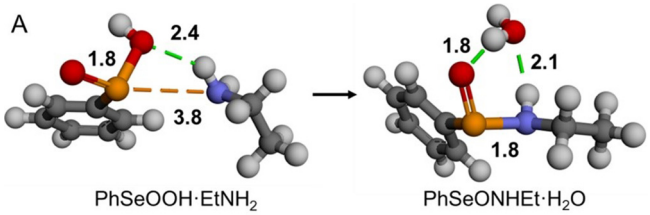

B

Molecule	Phase	
	Gas	Water
$PhSeOOH + EtNH_2$	0.0	0.0
$PhSeOOH{\cdot}EtNH_2$	-5.2	-1.1
$PhSeONHEt{\cdot}H_2O$	-11.1	-7.2
$PhSeONHEt + H_2O$	-0.9	-1.6

Fig. 5. The reaction of PSA with Lys residue model ($EtNH_2$) modeled at (PCM)-mPWPW91/def2PVTZ level of theory. (A) Intermolecular interactions of reagent and product complexes; the distances are in Å. (B) Energetics (kcal/mol) of the reaction in the gas and water phase. $PhSeOOH + EtNH_2$ and $PhSeONHEt + H_2O$ correspond to the reagents and products, while $PhSeOOH{\cdot}EtNH_2$ and $PhSeONHEt{\cdot}H_2O$ are the reactant and product complexes, respectively. All energy values are relative to the free reactants.

potential role of metabolites of a given drug can also be informative, as suggested by our present study. Organoselenium molecules have promising biological activity, and Ebselen is under clinical trials as potential lithium mimetic for bipolar disorder [120]. Of particular importance, Ebselen has been recently used against SARS-CoV-2 *in vitro* and presented antiviral activity possibly by inhibiting the main protease (Mpro) enzyme from the virus of COVID-19 [121]. Selenothymidines (selenium-containing AZT derivatives) are potential pharmacological agents against cancer [122]. DPDS presents many therapeutics properties (anxiolytic, antidepressant-like, anticancer, neuroprotective, and others) and its mechanism of action involves the modulation of the cellular redox status [123]. DPDS could modulate any protein having reactive thiol groups due to the lack of specific molecular targets. In this way, new DPDS derivatives with higher selectivity for specific protein targets still need to be developed.

4. Conclusion

The present work, entirely performed *in silico* and combining multiscale approaches, provides an efficient explanation to experimental *in vitro* data, giving evidence that DPDS inhibits *Hs*δ-AlaD and *Dm*δ-AlaD enzymes, but does not inhibit *Cs*δ-AlaD [11,29,30]. The molecular docking simulations between the selected organoselenium molecules and δ-AlaD could provide a possible explanation for this observation. The homology modeling showed that *Cs*δ-AlaD does not present Cys residues in the active site, and consequently, DPDS has not a substrate to oxidize. On the other hand, the putative metabolite PSA could access the active site, interacting with the Lys291 residue (Se···N), preventing the entrance of the 5-Ala substrate, and consequently inhibiting the *Cs*δ-AlaD. By DFT calculations, we have demonstrated that the reaction between PSA and Lys is indeed energetically favored. In *Hs*δ-AlaD and *Dm*δ-AlaD enzymes, both DPDS and PSA can access the active site, interacting with Cys124 (122), by Se···S interaction, which could lead to Cys oxidation, and, consequently, protein denaturation and enzyme inhibition. This type of study is essential to understand the reactivity and selectivity of organoselenium compounds in biological systems and can lead to better rational drug design. On the basis of these promising computational results, further studies are prompted. In addition, due to its protein similarity and organoselenium binding pose, *Dm*δ-AlaD rather than *Hs*δ-AlaD could be used as a model to test the toxicity of new organoselenium molecules.

CRediT authorship contribution statement

Pablo Andrei Nogara: Conceptualization, Methodology, Investigation, Validation, Writing - original draft. **Laura Orian:** Methodology, Resources, Writing - review & editing, Supervision, Funding acquisition. **João Batista Teixeira Rocha:** Methodology, Resources, Writing - review & editing, Supervision, Funding acquisition.

Declaration of Competing Interest

The authors declare that they have no known competing financial interests or personal relationships that could have appeared to influence the work reported in this paper.

Acknowledgments

The authors would like to thank the financial support by Coordination for Improvement of Higher Education Personnel CAPES/PROEX (n° 23038.005848/2018-31; n°0737/2018; n°88882.182123/2018-01), the CAPES/PrInt – Projeto Institucional de Internacionalização (n° 88887.374997/2019-00), the National Council for Scientific and Technological Development (CNPq), and the Rio Grande do Sul Foundation for Research Support (FAPERGS - Brazil). DFT calculations were carried out on Galileo (CINECA: Casalecchio di Reno, Italy) thanks to the ISCRA Grant HP10CUVVQU: "MEthylMErcury and Selenoproteins (MEMES).

Appendix A. Supplementary data

Supplementary data to this article can be found online at https://doi.org/10.1016/j.comtox.2020.100127.

References

[1] J.B.T. Rocha, B.C. Piccoli, C.S. Oliveira, Biological and chemical interest in selenium: a brief historical account, Arkivoc part ii (2017): 457–491. https://doi.org/10.3998/ark.5550190.p009.784.
[2] A.S. Weisberger, L.G. Suhrland, Studies on analogues of L-cysteine and L-cystine III. The effect of selenium cystine on Leukemia, Blood 11 (1956) 19–30.
[3] C.W. Nogueira, G. Zeni, J.B.T. Rocha, Organoselenium and organotellurium compounds: toxicology and pharmacology, Chem. Rev. 104 (2004) 6255–6285, https://doi.org/10.1021/cr0406559.
[4] C.W. Nogueira, J.B.T. Rocha, Toxicology and pharmacology of selenium: emphasis on synthetic organoselenium compounds, Arch. Toxicol. 85 (2011) 1313–1359, https://doi.org/10.1007/s00204-011-0720-3.
[5] G. Mugesh, H.B. Singh, Synthetic organoselenium compounds as antioxidants: glutathione peroxidase activity, Chem. Soc. Rev. 29 (2000) 347–357, https://doi.org/10.1039/a908114c.
[6] C. Santi, S. Santoro, B. Battistelli, Organoselenium compounds as catalysts in nature and laboratory, Curr. Org. Chem. 14 (2010) 2442–2462, https://doi.org/10.2174/138527210793358231.
[7] N.V. Barbosa, C.W. Nogueira, P.A. Nogara, A.F. De Bem, M. Aschner, J.B.T. Rocha, Organoselenium compounds as mimics of selenoproteins and thiol modifier agents, Metallomics 9 (2017) 1703–1734, https://doi.org/10.1039/c7mt00083a.
[8] D.M. Bissell, J.C. Lai, R.K. Meister, P.D. Blanc, Role of delta-aminolevulinic acid in the symptoms of acute porphyria, Am. J. Med. 128 (2015) 313–317, https://doi.org/10.1016/j.amjmed.2014.10.026.
[9] S. Sassa, ALAD porphyria, Semin. Liver Dis. 18 (1998) 95–101, https://doi.org/10.1055/s-2007-1007145.
[10] J.B.T. Rocha, R.A. Saraiva, S.C. Garcia, F.S. Gravina, C.W. Nogueira, Aminolevulinate dehydratase (δ-ALA-D) as marker protein of intoxication with metals and other pro-oxidant situations, Toxicol. Res. (Camb) 1 (2012) 85–102, https://doi.org/10.1039/c2tx20014g.
[11] C.W. Nogueira, V.C. Borges, G. Zeni, J.B.T. Rocha, Organochalcogens effects on d-aminolevulinate dehydratase activity from human erythrocytic cells in vitro, Toxicology 191 (2003) 169–178, https://doi.org/10.1016/S0300-483X(03)00250-6.
[12] E.K. Jaffe, The porphobilinogen synthase catalyzed reaction mechanism, Bioorg. Chem. 32 (2004) 316–325, https://doi.org/10.1016/j.bioorg.2004.05.010.
[13] E.K. Jaffe, The remarkable character of porphobilinogen synthase, Acc. Chem. Res. 49 (2016) 2509–2517, https://doi.org/10.1021/acs.accounts.6b00414.

[14] E.K. Jaffe, Porphobilinogen synthase, the first source of Heme's asymmetry, J. Bioenerg. Biomembr. 27 (1995) 169–179, https://doi.org/10.1007/BF02110032.
[15] E.K. Jaffe, S. Ali, L.W. Mitchell, K.M. Taylor, M. Volin, G.D. Markham, Characterization of the role of the stimulatory magnesium of escherichia coli porphobilinogen synthase, Biochemistry 34 (1995) 244–251, https://doi.org/10.1021/bi00001a029.
[16] I.U. Heinemann, M. Jahn, D. Jahn, The biochemistry of heme biosynthesis, Arch. Biochem. Biophys. 474 (2008) 238–251, https://doi.org/10.1016/j.abb.2008.02.015.
[17] G. Layer, J. Reichelt, D. Jahn, D.W. Heinz, Structure and function of enzymes in heme biosynthesis, Protein Sci. 19 (2010) 1137–1161, https://doi.org/10.1002/pro.405.
[18] N. Mills-Davies, D. Butler, E. Norton, D. Thompson, M. Sarwar, J. Guo, R. Gill, N. Azim, A. Coker, S.P. Wood, P.T. Erskine, L. Coates, J.B. Cooper, N. Rashid, M. Akhtar, P.M. Shoolingin-Jordan, Structural studies of substrate and product complexes of 5-aminolaevulinic acid dehydratase from humans, Escherichia coli and the hyperthermophile Pyrobaculum calidifontis, Acta Crystallogr. Sect. D Struct. Biol. 73 (2017) 9–21, https://doi.org/10.1107/S2059798316019525.
[19] P.T. Erskine, R. Newbold, A.A. Brindley, S.P. Wood, P.M. Shoolingin-Jordan, M.J. Warren, J.B. Cooper, The X-ray structure of yeast 5-aminolaevulinic acid dehydratase complexed with substrate and three inhibitors, J. Mol. Biol. 312 (2001) 133–141, https://doi.org/10.1006/jmbi.2001.4947.
[20] K.M. Cheung, P. Spencer, M.P. Timko, P.M. Shoolingin-Jordan, Characterization of a recombinant pea 5-aminolevulinic acid dehydratase and comparative inhibition studies with the Escherichia coli dehydratase, Biochemistry 36 (1997) 1148–1156, https://doi.org/10.1021/bi961215h.
[21] E.K. Jaffe, D. Shanmugam, A. Gardberg, S. Dieterich, B. Sankaran, L.J. Stewart, P.J. Myler, D.S. Roos, Crystal structure of Toxoplasma gondii porphobilinogen synthase: insights on octameric structure and porphobilinogen formation, J. Biol. Chem. 286 (2011) 15298–15307, https://doi.org/10.1074/jbc.M111.226225.
[22] A.B. Reitz, U.D. Ramirez, L. Stith, Y. Du, G.R. Smith, E.K. Jaffe, Pseudomonas aeruginosa porphobilinogen synthase assembly state regulators: hit discovery and initial SAR studies, Arkivoc 2010 (2010) 175–188, https://doi.org/10.3998/ark.5550190.0011.815.
[23] N.B.V. Barbosa, J.B.T. Rocha, G. Zeni, T. Emanuelli, M.C. Beque, A.L. Braga, Effect of organic forms of selenium on δ-aminolevulinate dehydratase from liver, kidney, and brain of adult rats, Toxicol. Appl. Pharmacol. 149 (1998) 243–253, https://doi.org/10.1006/taap.1998.8373.
[24] E.N. Maciel, R.C. Bolzan, A.L. Braga, J.B.T. Rocha, Diphenyl diselenide and diphenyl ditelluride differentially affect δ-aminolevulinate dehydratase from liver, kidney, and brain of mice, J. Biochem. Mol. Toxicol. 14 (2000) 310–319, https://doi.org/10.1002/1099-0461(2000)14:6<310::aid-jbt3>3.3.co;2-4.
[25] R. Fachinetto, L.A. Pivetta, M. Farina, R.P. Pereira, C.W. Nogueira, J.B.T. Rocha, Effects of ethanol and diphenyl diselenide exposure on the activity of δ-aminolevulinate dehydratase from mouse liver and brain, Food Chem. Toxicol. 44 (2006) 588–594, https://doi.org/10.1016/j.fct.2005.10.014.
[26] I.J. Kade, M.W. Paixão, O.E.D. Rodrigues, E.O. Ibukun, A.L. Braga, G. Zeni, C.W. Nogueira, J.B.T. Rocha, Studies on the antioxidant effect and interaction of diphenyl diselenide and dicholesteroyl diselenide with hepatic δ-aminolevulinic acid dehydratase and isoforms of lactate dehydrogenase, Toxicol. Vitr. 23 (2009) 14–20, https://doi.org/10.1016/j.tiv.2008.08.008.
[27] I.J. Kade, V.C. Borges, L. Savegnago, E.O. Ibukun, G. Zeni, C.W. Nogueira, J.B.T. Rocha, Effect of oral administration of diphenyl diselenide on antioxidant status, and activity of delta aminolevulinic acid dehydratase and isoforms of lactate dehydrogenase, in streptozotocin-induced diabetic rats, Cell Biol. Toxicol. 25 (2009) 415–424, https://doi.org/10.1007/s10565-008-9095-5.
[28] D.S. Ávila, A.L. Braga, I.J. Kade, N.B.V. Barbosa, J.B.T. Rocha, O.E.D. Rodrigues, C.W. Nogueira, M.W. Paixão, Comparative studies on dicholesteroyl diselenide and diphenyl diselenide as antioxidant agents and their effect on the activities of Na+/K+ ATPase and δ-aminolevulinic acid dehydratase in the rat brain, Neurochem. Res. 33 (2008) 167–178, https://doi.org/10.1007/s11064-007-9432-8.
[29] R.M. Golombieski, D.A.S. Graichen, L.A. Pivetta, C.W. Nogueira, E.L.S. Loreto, J.B.T. Rocha, Diphenyl diselenide [(PhSe)2] inhibits Drosophila melanogaster δ-aminolevulinate dehydratase (δ-ALA-D) gene transcription and enzyme activity, Comp. Biochem. Physiol. - C Toxicol. Pharmacol. 147 (2008) 198–204, https://doi.org/10.1016/j.cbpc.2007.09.007.
[30] M. Farina, N.B.V. Barbosa, C.W. Nogueira, V. Folmer, G. Zeni, L.H. Andrade, A.L. Braga, J.B.T. Rocha, Reaction of diphenyl diselenide with hydrogen peroxide and inhibition of delta-aminolevulinate dehydratase from rat liver and cucumber leaves, Brazilian J. Med. Biol. Res. 35 (2002) 623–631, https://doi.org/10.1590/S0100-879X2002000600001.
[31] R.J. Krause, S.C. Glocke, A.R. Sicuri, S.L. Ripp, A.A. Elfarra, Oxidative metabolism of seleno-L-methionine to L-methionine selenoxide by flavin-containing monooxygenases, Chem. Res. Toxicol. 19 (2006) 1643–1649, https://doi.org/10.1021/tx0601915.
[32] G.P. Chen, D.M. Ziegler, Liver microsome and flavin-containing monooxygenase catalyzed oxidation of organic selenium compounds, Arch. Biochem. Biophys. 312 (1994) 566–572, https://doi.org/10.1006/abbi.1994.1346.
[33] J.C. Madden, G. Pawar, M.T.D. Cronin, S. Webb, Y. Tan, A. Paini, In silico resources to assist in the development and evaluation of physiologically-based kinetic models, Comput. Toxicol. 11 (2019) 33–49, https://doi.org/10.1016/j.comtox.2019.03.001.
[34] R. Friedman, K. Boye, K. Flatmark, Molecular modelling and simulations in cancer research, Biochim. Biophys. Acta - Rev. Cancer. 2013 (1836) 1–14, https://doi.org/10.1016/j.bbcan.2013.02.001.
[35] R.A. Hodos, B.A. Kidd, K. Shameer, B.P. Readhead, J.T. Dudley, In silico methods for drug repurposing and pharmacology, Wiley Interdiscip. Rev. Syst. Biol. Med. 8 (2016) 186–210, https://doi.org/10.1002/wsbm.1337.
[36] A.B. Raies, V.B. Bajic, In silico toxicology: computational methods for the prediction of chemical toxicity, Wiley Interdiscip. Rev. Comput. Mol. Sci. 6 (2016) 147–172, https://doi.org/10.1002/wcms.1240.
[37] C.L. Mellor, F.P. Steinmetz, M.T.D. Cronin, Using molecular initiating events to develop a structural alert based screening work flow for nuclear receptor ligands associated with hepatic steatosis, Chem. Res. Toxicol. 29 (2016) 203–212, https://doi.org/10.1021/acs.chemrestox.5b00480.
[38] D.B. Kitchen, H. Decornez, J.R. Furr, J. Bajorath, Docking and scoring in virtual screening for drug discovery: methods and applications, Nat. Rev. Drug Discov. 3 (2004) 935–949, https://doi.org/10.1038/nrd1549.
[39] Y. Chen, Beware of docking!, Trends Pharmacol. Sci. 36 (2015) 78–95, https://doi.org/10.1016/j.tips.2014.12.001.
[40] R. Grzywa, E. Dyguda-Kazimierowicz, M. Sieńczyk, M. Feliks, W.A. Sokalski, J. Oleksyszyn, The molecular basis of urokinase inhibition: from the nonempirical analysis of intermolecular interactions to the prediction of binding affinity, J. Mol. Model. 13 (2007) 677–683, https://doi.org/10.1007/s00894-007-0193-8.
[41] T.L. Gonzalez, J.M. Rae, J.A. Colacino, R.J. Richardson, Homology models of mouse and rat estrogen receptor-α ligand-binding domain created by in silico mutagenesis of a human template: molecular docking with 17β-estradiol, diethylstilbestrol, and paraben analogs, Comput. Toxicol. 10 (2019) 1–16, https://doi.org/10.1016/j.comtox.2018.11.003.
[42] R.O. Jones, Density functional theory: its origins, rise to prominence, and future, Rev. Mod. Phys. 87 (2015) 897–923, https://doi.org/10.1103/RevModPhys.87.897.
[43] A.J. Cohen, P. Mori-Sánchez, W. Yang, Challenges for density functional theory, Chem. Rev. 112 (2012) 289–320, https://doi.org/10.1021/cr200107z.
[44] R.A. Saraiva, P.A. Nogara, R.F. Costa, E.M. Bezerra, H.N.H. Veras, I.R.A. Menezes, U.L. Fulco, E.L. Albuquerque, V.N. Freire, J.B.T. Rocha, Interaction energy profile for diphenyl diselenide in complex with δ-aminolevulinic acid dehydratase enzyme using quantum calculations and a molecular fragmentation method, Comput. Toxicol. 7 (2018) 9–19, https://doi.org/10.1016/j.comtox.2018.05.002.
[45] J. Carlsson, R.G. Coleman, V. Setola, J.J. Irwin, H. Fan, A. Schlessinger, A. Sali, B.L. Roth, B.K. Shoichet, Ligand discovery from a dopamine D3 receptor homology model and crystal structure, Nat. Chem. Biol. 7 (2011) 769–778, https://doi.org/10.1038/nchembio.662.
[46] K.S. Nascimento, D.A. Araripe, V.R. Pinto-Junior, V.J.S. Osterne, F.W.V. Martins, A.H.B. Neco, G.A. Farias, B.S. Cavada, Homology modeling, molecular docking, and dynamics of two α-methyl-d-mannoside-specific lectins from Arachis genus, J. Mol. Model. 24 (2018) 251, https://doi.org/10.1007/s00894-018-3800-y.
[47] J.L.R. Scaini, A.D. Camargo, V.R. Seus, A. von Groll, A.V. Werhli, P.E.A. da Silva, K. dos S. Machado, Molecular modelling and competitive inhibition of a Mycobacterium tuberculosis multidrug-resistance efflux pump, J. Mol. Graph. Model. 87 (2019) 98–108, https://doi.org/10.1016/j.jmgm.2018.11.016.
[48] J.H. Kim, S.K. Kim, J.H. Lee, Y.J. Kim, W.A. Goddard, Y.C. Kim, Homology modeling and molecular docking studies of Drosophila and Aedes sex peptide receptors, J. Mol. Graph. Model. 66 (2016) 115–122, https://doi.org/10.1016/j.jmgm.2016.03.014.
[49] Å Mortensen, S. Mæhre, K. Kristiansen, E.S. Heimstad, G.W. Gabrielsen, B.M. Jenssen, I. Sylte, Homology modeling to screen for potential binding of contaminants to thyroid hormone receptor and transthyretin in glaucous gull (Larus hyperboreus) and herring gull (Larus argentatus), Comput. Toxicol. 13 (2020): 100120. https://doi.org/10.1016/j.comtox.2020.100120.
[50] J. He, D. Li, K. Xiong, Y. Ge, H. Jin, G. Zhang, M. Hong, Y. Tian, J. Yin, H. Zeng, Inhibition of thioredoxin reductase by a novel series of bis-1,2-benzisoselenazol-3(2H)-ones: organoselenium compounds for cancer therapy, Bioorganic Med. Chem. 20 (2012) 3816–3827, https://doi.org/10.1016/j.bmc.2012.04.033.
[51] P.A. Nogara, J.B.T. Rocha, In silico studies of mammalian δ-ALAD interactions with selenides and selenoxides, Mol. Inform. 36 (2017) 1–8, https://doi.org/10.1002/minf.201700091.
[52] L. Orian, S. Toppo, Organochalcogen peroxidase mimetics as potential drugs: a long story of a promise still unfulfilled, Free Radic. Biol. Med. 66 (2014) 65–74, https://doi.org/10.1016/j.freeradbiomed.2013.03.006.
[53] L.P. Wolters, L. Orian, Peroxidase activity of organic selenides: mechanistic insights from quantum chemistry, Curr. Org. Chem. 20 (2016) 189–197, https://doi.org/10.2174/1385272819666150724233655.
[54] E. Fragoso, R. Azpiroz, P. Sharma, G. Espinosa-Pérez, F. Lara-Ochoa, A. Toscano, R. Gutierrez, O. Portillo, New organoselenium compounds with intramolecular Se···O/ Se···H interactions: NMR and theoretical studies, J. Mol. Struct. 1155 (2018) 711–719, https://doi.org/10.1016/j.molstruc.2017.11.054.
[55] C.A. Bayse, B.D. Allison, Activation energies of selenoxide elimination from Se-substituted selenocysteine, J. Mol. Model. 13 (2007) 47–53, https://doi.org/10.1007/s00894-006-0128-9.
[56] L. Orian, P. Mauri, A. Roveri, S. Toppo, L. Benazzi, V. Bosello-Travain, A. De Palma, M. Maiorino, G. Miotto, M. Zaccarin, A. Polimeno, L. Flohé, F. Ursini, Selenocysteine oxidation in glutathione peroxidase catalysis: an MS-supported quantum mechanics study, Free Radic. Biol. Med. 87 (2015) 1–14, https://doi.org/10.1016/j.freeradbiomed.2015.06.011.
[57] M. Bortoli, M. Torsello, F.M. Bickelhaupt, L. Orian, Role of the chalcogen (S, Se, Te) in the oxidation mechanism of the glutathione peroxidase active site, ChemPhysChem 18 (2017) 2990–2998, https://doi.org/10.1002/cphc.201700743.
[58] M.D. Tiezza, G. Ribaudo, L. Orian, Organodiselenides: organic catalysis and drug design learning from glutathione peroxidase, Curr. Org. Chem. 23 (2019)

1381–1402, https://doi.org/10.2174/1385272822666180803123137.
[59] K. Arnold, L. Bordoli, J. Kopp, T. Schwede, The SWISS-MODEL workspace: a web-based environment for protein structure homology modelling, Bioinformatics 22 (2006) 195–201, https://doi.org/10.1093/bioinformatics/bti770.
[60] L.A. Kelly, S. Mezulis, C. Yates, M. Wass, M. Sternberg, The Phyre2 web portal for protein modelling, prediction, and analysis, Nat. Protoc. 10 (2015) 845–858, https://doi.org/10.1038/nprot.2015-053.
[61] C. Combet, M. Jambon, G. Deléage, C. Geourjon, Geno3D: automatic comparative molecular modelling of protein, Bioinformatics 18 (2002) 213–214, https://doi.org/10.1093/bioinformatics/18.1.213.
[62] L. Coates, G. Beaven, P.T. Erskine, S.I. Beale, S.P. Wood, P.M. Shoolingin-Jordan, J.B. Cooper, Structure of Chlorobium vibrioforme 5-aminolaevulinic acid dehydratase complexed with a diacid inhibitor, Acta Crystallogr. Sect. D Biol. Crystallogr. 61 (2005) 1594–1598, https://doi.org/10.1107/S0907444905030350.
[63] F. Frère, W.D. Schubert, F. Stauffer, N. Frankenberg, R. Neier, D. Jahn, D.W. Heinz, Structure of porphobilinogen synthase from pseudomonas aeruginosa in complex with 5-fluorolevulinic acid suggests a double schiff base mechanism, J. Mol. Biol. 320 (2002) 237–247, https://doi.org/10.1016/S0022-2836(02)00472-2.
[64] E.K. Jaffe, J. Kervinen, J. Martins, F.R. Stauffer, R. Neier, A. Wlodawer, A. Zdanov, Species-specific inhibition of porphobilinogen synthase by 4-oxosebacic acid, J. Biol. Chem. 277 (2002) 19792–19799, https://doi.org/10.1074/jbc.M201486200.
[65] D. Eisenberg, R. Luthy, J.U. Bowie, VERIFY 3D: assessment of protein models with three-dimensional profiles, Methods Enzymol. 277 (1997) 396–404.
[66] J.U. Bowie, R. Luthy, D. Eisenberg, A method to identify protein sequences that fold into a known three-dimensional structure, Science (80-.). 253 (1991): 164–170. https://doi.org/10.1126/science.1853201.
[67] M. Wiederstein, M.J. Sippl, ProSA-web: interactive web service for the recognition of errors in three-dimensional structures of proteins, Nucleic Acids Res. 35 (2007) 407–410, https://doi.org/10.1093/nar/gkm290.
[68] R.A. Laskowski, M.W. MacArthur, D.S. Moss, J.M. Thornton, PROCHECK: a program to check the stereochemical quality of protein structures, J. Appl. Crystallogr. 26 (1993) 283–291, https://doi.org/10.1107/S0021889892009944.
[69] G.N. Ramachandran, V. Sasisekharan, Conformation of polypeptides and proteins, Adv. Protein Chem. 23 (1968) 283–438, https://doi.org/10.1016/S0065-3233(08)60402-7.
[70] C. Colovos, T.O. Yeates, Verification of protein structures: patterns of nonbonded atomic interactions, Protein Sci. 2 (1993) 1511–1519, https://doi.org/10.1002/pro.5560020916.
[71] R.A. Laskowski, PDBsum: summaries and analyses of PDB structures, Nucleic Acids Res. 29 (2001) 221–222, https://doi.org/10.1093/nar/29.1.221.
[72] N. Mills-Davies, D. Thompson, J. Cooper, S. Wood, P.M. Shoolingin-Jordan, Crystal structure of native human erythrocyte 5-aminolaevulinic acid dehydratase, RCSB PDB (2000), https://doi.org/10.2210/pdb1E51/pdb.
[73] E.F. Pettersen, T.D. Goddard, C.C. Huang, G.S. Couch, D.M. Greenblatt, E.C. Meng, T.E. Ferrin, UCSF Chimera - a visualization system for exploratory research and analysis, J. Comput. Chem. 25 (2004) 1605–1612, https://doi.org/10.1002/jcc.20084.
[74] M.D. Hanwell, D.E. Curtis, D.C. Lonie, T. Vandermeersch, E. Zurek, G.R. Hutchison, Avogadro: an advanced semantic chemical editor, visualization, and analysis platform, J. Cheminform. 4 (2012) 1–17, https://doi.org/10.1186/1758-2946-4-17.
[75] J.J.P. Stewart, Optimization of parameters for semiempirical methods V: Modification of NDDO approximations and application to 70 elements, J. Mol. Model. 13 (2007) 1173–1213, https://doi.org/10.1007/s00894-007-0233-4.
[76] J.D. McCullough, E.S. Gould, The dissociation constants of some mono-substituted benzeneseleninic acids, J. Am. Chem. Soc. 71 (1949) 674–676, https://doi.org/10.1021/ja01170a083.
[77] G.M. Morris, R. Huey, W. Lindstrom, M.F. Sanner, R.K. Belew, D.S. Goodsell, A.J. Olson, AutoDock4 and AutoDockTools4: automated docking with selective receptor flexibility, J. Comput. Chem. 30 (2009) 2785–2791, https://doi.org/10.1002/jcc.21256.
[78] O. Trott, A.J. Olson, AutoDock Vina: improving the speed and accuracy of docking with a new scoring function, efficient optimization, and multithreading, J. Comput. Chem. 31 (2010) 455–461, https://doi.org/10.1002/jcc.21334.
[79] J.L. Stigliani, V. Bernardes-Génisson, J. Bernadou, G. Pratviel, Cross-docking study on InhA inhibitors: a combination of Autodock Vina and PM6-DH2 simulations to retrieve bio-active conformations, Org. Biomol. Chem. 10 (2012) 6341–6349, https://doi.org/10.1039/c2ob25602a.
[80] C.P. Vianna, W.F. De Azevedo, Identification of new potential Mycobacterium tuberculosis shikimate kinase inhibitors through molecular docking simulations, J. Mol. Model. 18 (2012) 755–764, https://doi.org/10.1007/s00894-011-1113-5.
[81] M.J. Frisch, G.W. Trucks, H.B. Schlegel, G.E. Scuseria, M.A. Robb, J.R. Cheeseman, G. Scalmani, V. Barone, G.A. Petersson, H. Nakatsuji, X. Li, M. Caricato, A. Marenich, J. Bloino, B.G. Janesko, R. Gomperts, B. Mennucci, H.P. Hratchian, J.V. Ortiz, A.F. Izmaylov, J.L. Sonnenberg, D. Williams-Young, F. Ding, F. Lipparini, F. Egidi, J. Goings, B. Peng, A. Petrone, T. Henderson, D. Ranasinghe, V.G. Zakrzewski, J. Gao, N. Rega, G. Zheng, W. Liang, M. Hada, M. Ehara, K. Toyota, R. Fukuda, J. Hasegawa, M. Ishida, T. Nakajima, Y. Honda, O. Kitao, H. Nakai, T. Vreven, K. Throssell, J.A. Montgomery Jr., J.E. Peralta, F. Ogliaro, M. Bearpark, J.J. Heyd, E. Brothers, K.N. Kudin, V.N. Staroverov, T. Keith, R. Kobayashi, J. Normand, K. Raghavachari, A. Rendell, J.C. Burant, S.S. Iyengar, J. Tomasi, M. Cossi, J.M. Millam, V. Klene, C. Adamo, R. Cammi, V. Ochterski, R.L. Martin, K. Morokuma, O. Farkas, J.B. Foresman, D.J. Fox, Gaussian 09 (2009).
[82] C. Adamo, V. Barone, Exchange functionals with improved long-range behavior and adiabatic connection methods without adjustable parameters: the mPW and mPW1PW models, J. Chem. Phys. 108 (1998) 664–675, https://doi.org/10.1063/1.475428.
[83] T.H. Dunning, Gaussian basis functions for use in molecular calculations. IV. The representation of polarization functions for the first row atoms and hydrogen, J. Chem. Inf. Model. 55 (1971): 3958–3966. https://doi.org/10.1063/1.1676685.
[84] S. Antony, C.A. Bayse, Modeling the mechanism of the glutathione peroxidase mimic ebselen, Inorg. Chem. 50 (2011) 12075–12084, https://doi.org/10.1021/ic201603v.
[85] J. Tomasi, B. Mennucci, R. Cammi, Quantum mechanical continuum solvation models, Chem. Rev. 105 (2005) 2999–3094, https://doi.org/10.1021/cr9904009.
[86] J. Kervinen, E.K. Jaffe, F. Stauffer, R. Neier, A. Wlodawer, A. Zdanov, Mechanistic basis for suicide inactivation of porphobilinogen synthase by 4,7-Dioxosebacic acid, an inhibitor that shows dramatic species selectivity, Biochemistry 40 (2001) 8227–8236, https://doi.org/10.1021/bi010656k.
[87] V.K. Vyas, R.D. Ukawala, M. Ghate, C. Chintha, homology modeling a fast tool for drug discovery: current perspectives, Indian J. Pharm. Sci. 74 (2012) 1–17.
[88] T. Schmidt, A. Bergner, T. Schwede, Modelling three-dimensional protein structures for applications in drug design, Drug Discov. Today. 19 (2014) 890–897, https://doi.org/10.1016/j.drudis.2013.10.027.
[89] Z. Xiang, Advances in homology protein structure modeling, Curr. Protein Pept. Sci. 7 (2006) 217–227, https://doi.org/10.2174/138920306777452312.
[90] E. Erdtman, E.A.C. Bushnell, J.W. Gauld, L.A. Eriksson, Computational insights into the mechanism of porphobilinogen synthase, J. Phys. Chem. B. 114 (2010) 16860–16870, https://doi.org/10.1021/jp103590d.
[91] C.S. Lentz, D. Stumpfe, J. Bajorath, M. Famulok, A. Hoerauf, K.M. Pfarr, New chemotypes for wALADin1-like inhibitors of delta-aminolevulinic acid dehydratase from Wolbachia endobacteria, Bioorganic Med. Chem. Lett. 23 (2013) 5558–5562, https://doi.org/10.1016/j.bmcl.2013.08.052.
[92] C.S. Lentz, V. Halls, J.S. Hannam, B. Niebel, U. Strübing, G. Mayer, A. Hoerauf, M. Famulok, K.M. Pfarr, A selective inhibitor of heme biosynthesis in endosymbiotic bacteria elicits antifilarial activity in vitro, Chem. Biol. 20 (2013) 177–187, https://doi.org/10.1016/j.chembiol.2012.11.009.
[93] B. Wu, J. Novelli, J. Foster, R. Vaisvila, L. Conway, J. Ingram, M. Ganatra, A.U. Rao, I. Hamza, B. Slatko, The heme biosynthetic pathway of the obligate wolbachia endosymbiont of brugia malayi as a potential anti-filarial drug target, PLoS Negl. Trop. Dis. 3 (2009) e475, https://doi.org/10.1371/journal.pntd.0000475.
[94] P.S. Kumar, Y.N. Kumar, U.V. Prasad, S. Yeswanth, V. Swarupa, G. Sowjenya, K. Venkatesh, L. Srikanth, V.K. Rao, P.V. Sarma, In silico designing and molecular docking of a potent analog against Staphylococcus aureus porphobilinogen synthase, J. Pharm. Bioallied Sci. 6 (2014) 158–166, https://doi.org/10.4103/0975-7406.135246.
[95] K.K. Mishra, S.K. Singh, P. Ghosh, D. Ghosh, A. Das, The nature of selenium hydrogen bonding: gas phase spectroscopy and quantum chemistry calculations, Phys. Chem. Chem. Phys. 19 (2017) 24179–24187, https://doi.org/10.1039/c7cp05265k.
[96] V.R. Mundlapati, D.K. Sahoo, S. Ghosh, U.K. Purame, S. Pandey, R. Acharya, N. Pal, P. Tiwari, H.S. Biswal, Spectroscopic evidences for strong hydrogen bonds with selenomethionine in proteins, J. Phys. Chem. Lett. 8 (2017) 794–800, https://doi.org/10.1021/acs.jpclett.6b02931.
[97] G. Ribaudo, M. Bellanda, I. Menegazzo, L.P. Wolters, M. Bortoli, G. Ferrer-Sueta, G. Zagotto, L. Orian, Mechanistic insight into the oxidation of organic phenylselenides by H2O2, Chem. - A Eur. J. 23 (2017) 2405–2422, https://doi.org/10.1002/chem.201604915.
[98] C.V. Klimaczewski, P.A. Nogara, N.V. Barbosa, J.B.T. da Rocha, Interaction of metals from group 10 (Ni, Pd, and Pt) and 11 (Cu, Ag, and Au) with human blood δ-ALA-D: in vitro and in silico studies, Environ. Sci. Pollut. Res. 25 (2018) 30557–30566, https://doi.org/10.1007/s11356-018-3048-1.
[99] P.B. Lutz, C.A. Bayse, Chalcogen bonding interactions between reducible sulfur and selenium compounds and models of zinc finger proteins, J. Inorg. Biochem. 157 (2016) 94–103, https://doi.org/10.1016/j.jinorgbio.2016.01.013.
[100] K.N. Sands, T.G. Back, Key steps and intermediates in the catalytic mechanism for the reduction of peroxides by the antioxidant ebselen, Tetrahedron 74 (2018) 4959–4967, https://doi.org/10.1016/j.tet.2018.05.027.
[101] M. Abdo, Z. Sun, S. Knapp, Biohybrid-Se-S-coupling reactions of an amino acid derived seleninate, Molecules 18 (2013) 1963–1972, https://doi.org/10.3390/molecules18021963.
[102] L. Engman, D. Stern, Thiol/diselenide exchange for the generation of benzeneselenolate ion. catalytic reductive ring-opening of α,β-epoxy ketoness, J. Org. Chem. 59 (1994): 5179–5183. https://doi.org/10.1021/jo00097a019.
[103] R.M. Rosa, R. Roesler, A.L. Braga, J. Saffi, J.A.P. Henriques, Pharmacology and toxicology of diphenyl diselenide in several biological models, Brazilian J. Med. Biol. Res. 40 (2007) 1287–1304, https://doi.org/10.1590/S0100-879X2006005000171.
[104] Y. Xue, X. Xia, B. Yu, L. Tao, Q. Wang, S.W. Huang, F. Yu, Selenylsulfide bond-launched reduction-responsive superparamagnetic nanogel combined of acid-responsiveness for achievement of efficient therapy with low side effect, ACS Appl. Mater. Interfaces 9 (2017) 30253–30257, https://doi.org/10.1021/acsami.7b06818.
[105] M. Kunstelj, K. Fidler, Š. Škrajnar, M. Kenig, V. Smilović, M. Kusterle, S. Caserman, I. Zore, V.G. Porekar, S. Jevševar, Cysteine-specific PEGylation of rhG-CSF via selenylsulfide bond, Bioconjug. Chem. 24 (2013) 889–896, https://doi.org/10.1021/bc3005232.
[106] D. Steinmann, T. Nauser, W.H. Koppenol, Selenium and sulfur in exchange reactions: a comparative study, J. Org. Chem. 75 (2010) 6696–6699, https://doi.org/

10.1021/jo1011569.
[107] M. Bortoli, L.P. Wolters, L. Orian, F.M. Bickelhaupt, Addition-elimination or nucleophilic substitution? Understanding the energy profiles for the reaction of chalcogenolates with dichalcogenides, J. Chem. Theory Comput. 12 (2016) 2752–2761, https://doi.org/10.1021/acs.jctc.6b00253.
[108] J.L. Kice, T.W.S. Lee, Oxidation-reduction reactions of organoselenium compounds. 1. Mechanism of the reaction between seleninic acids and thiols, J. Am. Chem. Soc. 100 (1978): 5094–5102. https://doi.org/10.1021/ja00484a031.
[109] P. Prabhu, B.G. Singh, M. Noguchi, P.P. Phadnis, V.K. Jain, M. Iwaoka, K.I. Priyadarsini, Stable selones in glutathione-peroxidase-like catalytic cycle of selenonicotinamide derivative, Org. Biomol. Chem. 12 (2014) 2404–2412, https://doi.org/10.1039/c3ob42336k.
[110] B.K. Sarma, G. Mugesh, Antioxidant activity of the anti-inflammatory compound ebselen: a reversible cyclization pathway via selenenic and seleninic acid intermediates, Chem. Eur. J. 14 (2008) 10603–10614, https://doi.org/10.1002/chem.200801258.
[111] G.R. Haenen, B.M. De Rooij, N.P. Vermeulen, A. Bast, Mechanism of the reaction of ebselen with endogenous thiols: dihydrolipoate is a better cofactor than glutathione in the peroxidase activity of ebselen, Mol. Pharmacol. 37 (1990) 412–422.
[112] W. Hassan, J.B. Teixeira Rocha, Interaction profile of diphenyl diselenide with pharmacologically significant thiols, Molecules 17 (2012) 12287–12296, https://doi.org/10.3390/molecules171012287.
[113] J. Chiou, S. Wan, K.F. Chan, P.K. So, D. He, E.W.C. Chan, T.H. Chan, K.Y. Wong, J. Tao, S. Chen, Ebselen as a potent covalent inhibitor of New Delhi metallo-β-lactamase (NDM-1), Chem. Commun. 51 (2015) 9543–9546, https://doi.org/10.1039/c5cc02594j.
[114] R.A. Saraiva, D.C. Bueno, P.A. Nogara, J.B.T. Rocha, Molecular docking studies of disubstituted diaryl diselenides as mammalian δ -aminolevulinic acid dehydratase enzyme inhibitors, J. Toxicol. Environ. Heal. Part A 75 (2012) 1012–1022, https://doi.org/10.1080/15287394.2012.697810.
[115] H.J. Reich, R.J. Hondal, Why nature chose selenium, ACS Chem. Biol. 11 (2016) 821–841, https://doi.org/10.1021/acschembio.6b00031.
[116] C. Santi, C. Tidei, Electrophilic selenium/tellurium reagents: reactivity and their contribution to green chemistry, in: PATAI'S Chem. Funct. Groups, 2013, pp. 1–87. https://doi.org/10.1002/9780470682531.pat0720.
[117] V.P. Singh, H.B. Singh, R.J. Butcher, Synthesis and glutathione peroxidase-like activities of isoselenazolines, Eur. J. Org. Chem. 3 (2011) 5485–5497, https://doi.org/10.1002/ejoc.201100899.
[118] T.G. Back, B.P. Dyck, A novel camphor-derived selenamide that acts as a glutathione peroxidase mimetic, J. Am. Chem. Soc. 119 (1997) 2079–2083, https://doi.org/10.1021/ja963602k.
[119] H.J. Reich, C.P. Jasperse, Organoselenium chemistry. Redox chemistry of selenocysteine model systems, J. Am. Chem. Soc. 109 (1987): 5549–5551. https://doi.org/10.1021/ja00252a055.
[120] N. Singh, A.C. Halliday, J.M. Thomas, O. Kuznetsova, R. Baldwin, E.C.Y. Woon, P.K. Aley, I. Antoniadou, T. Sharp, S.R. Vasudevan, G.C. Churchill, A safe lithium mimetic for bipolar disorder, Nat. Commun. 4 (2013) 1332–1337, https://doi.org/10.1038/ncomms2320.
[121] Z. Jin, X. Du, Y. Xu, Y. Deng, M. Liu, Y. Zhao, B. Zhang, X. Li, L. Zhang, C. Peng, Y. Duan, J. Yu, L. Wang, K. Yang, F. Liu, R. Jiang, X. Yang, T. You, X. Liu, X. Yang, F. Bai, H. Liu, X. Liu, L.W. Guddat, W. Xu, G. Xiao, C. Qin, Z. Shi, H. Jiang, Z. Rao, H. Yang, Structure of Mpro from COVID-19 virus and discovery of its inhibitors, Nature (2020), https://doi.org/10.1038/s41586-020-2223-y.
[122] M.S. Wagner, E. Schultze, T.L. Oliveira, P.M.M. de Leon, H.S. Thurow, V.F. Campos, I. Oliveira, D. de Souza, O.E.D. Rodrigues, T. Collares, F.K. Seixas, Revitalizing the AZT through of the selenium: an approach in human triple negative breast cancer cell line, Front. Oncol. 8 (2018) 525, https://doi.org/10.3389/fonc.2018.00525.
[123] P.A. Nogara, C.S. Oliveira, J.B.T. Rocha, Chemistry and pharmacology of synthetic organoselenium compounds, in: B.C. Ranu, B. Banerjee (Eds.), Organoselenium Chem., De Gruyter, Berlin, 2020, pp. 305–346. https://doi.org/10.1515/9783110625110-008.